*Proc. of the 2019 IEEE 6th International Conference on Smart Instrumentation, Measurement and Applications (ICSIMA 2019)*
*27-29 August 2019, Kuala Lumpur, Malaysia*

# Geometrical Analysis of Diffuser-Nozzle Elements for Valveless Micropumps

Marwan Nafea[#1], Mohamed Sultan Mohamed Ali[*2], Tariq Rehman[*3], Kamyar Mehranzamir[#4]

[#]*Department of Electrical and Electronic Engineering, Faculty of Science and Engineering, University of Nottingham Malaysia*
*43500 Semenyih, Selangor, Malaysia*

[*]*School of Electrical Engineering, Faculty of Engineering, Universiti Teknologi Malaysia*
*81310 Skudai, Johor, Malaysia*

[1]marwan.nafea@nottingham.edu.my (Corresponding author), [2]sultan_ali@fke.utm.my, [3]rtariq2@live.utm.my,
[4]kamyar.mehranzamir@nottingham.edu.my

***Abstract*—This paper reports a geometrical analysis and tuning-approach for diffuser-nozzle elements for valveless micropumps. Finite element analysis studies are performed in order to investigate the impact of the angle, curvature ratio, and length of the diffuser on the pumping efficiency. Parametric sweep studies are implemented at Reynolds number (*Re*) values ranging from 10 to 100 while observing the pressure coefficients in the nozzle and diffuser directions, as well as the flow separation and the resultant efficiency of the diffuser. The results suggest that a diffuser with an angle of 10° and a curvature ratio of 0.4 possesses the highest efficiency among the other diffusers within the *Re* range of this study. In addition, it is observed that the length of the diffuser has a positive effect on the efficiency, where the length is usually restricted by the overall size of the device. The results provide comprehensive designing guidelines for diffusers elements that can be used in microfluidic devices for various biomedical applications.**

***Keywords—diffuser; nozzle; valveless; micropump; finite element analysis***

## I. INTRODUCTION

Microelectromechanical systems (MEMS) is a promising technology that has enabled manufacturing a wide range of miniaturized devices using microfabrication techniques [1]. Since the beginning of the development in MEMS, fluidic devices caught the attention of researchers, which made them among the first devices to be fabricated in microscale. The most common fluidic devices were micropumps, which emerged from MEMS-technology as a favorable research field, due to their wide ranges of applications in space exploration, medicine, biology, and microelectronics cooling [2]. The first MEMS-based micropump was proposed by Smits in 1984. Since then, several types of MEMS-based micropumps have been reported to address the matters of transporting and pumping fluids at rates of few microliters per minute. One of the essential characteristics of micropumps is their ability of flow rectification to achieve a unidirectional stream. This can be achieved using a microvalve or a diffuser-nozzle element in the structure of the micropump [3]. Microvalves can be classified as active and passive types. Active microvalves are operated through the actuation of a membrane or a flap, while passive microvalves rely on the pressure drop between the inlet and outlet in order to rectify the flow [4]. A diffuser-nozzle element is a fluidic channel with inclined side walls that causes the fluidic resistance to be higher in one direction than the other, which consequently leads to a higher flow rate towards the lowest resistance side [5]. Thus, the function of the diffuser is transforming the kinetic energy of the fluid (flow velocity) to a potential energy (pressure). The concept of a valveless diffuser-nozzle micropump was first proposed by Stemme and Stemme in 1993. Since then, it has been widely adopted in micropumps designs, due to its several advantages over microvalves structures. The diffuser-nozzle structure offers a higher flow controllability, a simpler design and reduces the fabrication and packaging processes, and the power consumption required for microvalves structures [6]. In addition, the problems existing in microvalves structures, including wear, clogging and fatigue-induced failure can be eliminated when using diffuser-nozzle structures [1]. These features offer a simpler integration process in several biomedical applications, such as point of care testing, micro total analysis systems, lab-on-a-chip, and portable electroencephalography-controlled systems for drug delivery [7].

Several diffuser-nozzle models, such as pyramidal, conical, and planar were used for valveless micropumps [8]. The selection of the profile of the diffuser relies on the microfabrication method. Planar diffuser-nozzle designs are highly compliant with planar photolithography and conventional methods of micromachining [9]. In addition, when applying similar inlet conditions, the best planar profiles can be up to 80% shorter than the best conical profiles. Thus, several studies on diffuser-nozzle element have design and optimization been carried out [10]. However, it is necessary to investigate the impact of several fluid and geometric parameters on the flow inside diffuser-nozzle element. With the continuous miniaturization of micropumps, the performance of these devices is increasingly affected by the diffusers elements designs.

Motivated by the aforementioned issues, this paper presents a comprehensive analysis on the effect of geometry of the diffuser-nozzle on the pumping performance. The design and working principle of the diffuser-nozzle is presented. Then, a finite element analysis (FEA) with parametric studies is carried

This work was supported by the University of Nottingham Malaysia, Prototype Research Grant Scheme (PRGS) 4L690 by the Ministry of Education Malaysia, and UTM Shine 04G75 by Universiti Teknologi Malaysia.

out at various Reynolds number (*Re*) values, while varying the angle ($\theta$), curvature ratio (*CR*), and length (*L*) of the diffuser.

## II. Design and Working Principle

This section investigates the diffuser-nozzle pressure drop coefficients. The diffuser-nozzle design schematic is shown in Fig. 1. The diffuser is connected between two microchannels with areas of $A_i$ and $A_o$. The areas of the inlet and outlet of the diffuser are donated by $A_{din}$ and $A_{dout}$, respectively, with respective widths of $w_1$ and $w_2$. The fluid flow in the diffuser direction is considered as a positive flow, while the flow in the nozzle direction is considered as a negative flow. The incompressible flow energy equation for a fluid flowing the diffuser can be described as follows [11]:

$$p_i + \frac{1}{2}\alpha_i \rho \overline{V_i^2} = p_o + \frac{1}{2}\alpha_o \rho \overline{V}_e^2 + \Delta p_{i-o} \tag{1}$$

where $p_i$ is the hydrostatic pressure across the section, $\rho$ is the fluid density, $\overline{V}$ is the volumetric average velocity, and $\alpha$ is the kinetic energy correction factor, which is given as:

$$\alpha = \frac{1}{A\overline{V}^3}\int_A u^3 \mathrm{d}A \tag{2}$$

where $u$ is the axial velocity of the fluid. In the positive flow direction, the pressure drop between the inlet and outlet is caused by the inlet, diffuser, and outlet pressure losses. This can be represented as [12]:

$$\Delta p_{i-o} = \Delta p_{i-din} + \Delta p_{din-dout} + \Delta p_{dout-o} \tag{3}$$

The loss coefficient between the inlet to the outlet sections, $K_{io}$, is given as:

$$K_{io} = \frac{2\Delta p_{i-o}}{\rho V_{din}^2} \tag{4}$$

Based on (1-4), the pressure coefficient of the diffuser, $\xi_d$, can be defined as:

$$\xi_d = \frac{2(p_i - p_o)}{\rho V_1^2} + c_i\left(\frac{A_{din}}{A_i}\right)^2 - c_o\left(\frac{A_{din}}{A_o}\right)^2 \tag{5}$$

Since $A_i$, $A_o >> A_{din}$, the pressure coefficients of the diffuser and the nozzle directions can be represented as:

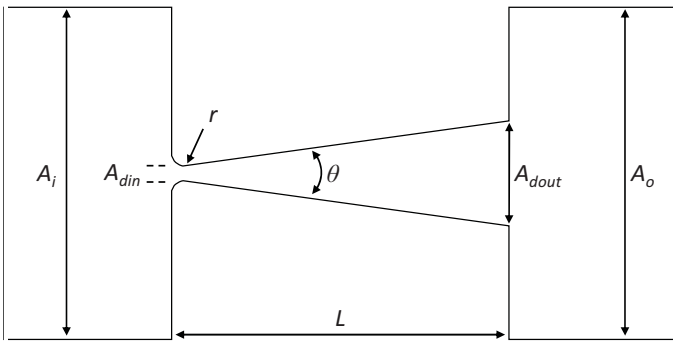


Fig. 1. Schematic of a diffuser-nozzle of a micropump.

$$\xi_d = \frac{2(p_i - p_o)}{\rho V_{din}^2} \tag{6}$$

$$\xi_n = \frac{2(p_o - p_i)}{\rho V_{din}^2} \tag{7}$$

The ratio of the latter to the former is known as the efficiency of the diffuser, which can be presented as follows:

$$\eta = \frac{\xi_n}{\xi_d} \tag{8}$$

In order to direct the flow towards the outlet, a practical diffuser must have an efficiency greater than 1. The volumetric efficiency of a symmetric diffuser-based micropump can be represented as:

$$\varepsilon = V_p\left(\frac{\sqrt{\eta}-1}{\sqrt{\eta}+1}\right) \tag{9}$$

where $V_p$ is the dynamic constant of the micropump. Equation (9) states that the efficiency of a diffuser-based micropump is increased when increasing the efficiency of the diffuser-nozzle structure [4]. Previous studies investigated the effect of several factors on the performance of the diffuser. Such factors include the angle of the diffuser, slenderness (diffuser length/inlet width), area ratio (outlet area/inlet area), inlet aspect ratio (inlet depth/inlet width), relative throat edge radius (throat radius/hydraulic diameter), and *Re*, which is expressed as follows:

$$Re = \frac{\rho \overline{V} d}{\mu} \tag{10}$$

where $d$ is the hydraulic diameter of the microchannel and $\mu$ is the dynamic viscosity of the liquid. This research focuses on investigating the impact of the angle, length, and curvature ratio (the ratio of the inlet fillet radius to the opening throat width) of the diffuser on the losses and efficiency of the diffuser.

## III. Finite Element Analysis

In this work, COMSOL Multiphysics® was used to perform the numerical simulation of a two-dimensional (2D) model of the diffuser. To reduce the complexity of the model and reduce the simulation time, only a half of the diffuser was simulated, since the geometry of the diffuser is symmetrical. Thus, the angle of this half of the diffuser is half the angle of the complete diffuser ($\theta$) that is presented in in Fig. 1, which means that it should be doubled when presenting the results. In the simulation process, two laminar flow physics were used to represent the flow of the fluid in the diffuser and nozzle directions. No-slip boundary conditions were implemented on the walls, except the inlet and outlet boundaries. The inlet boundary was set to a velocity input that varies accordingly with *Re* values, while zero-gauge pressure was set at the outlet boundary layer. The boundary conditions of the inlet and outlet were inversed in the two laminar flow physics. To guarantee the independency of the results of the analysis, a mesh

sensitivity test with different mesh densities was carried out [13]. A PARDISO solver was used to achieve a fast solution convergence and reduce the numerical error that is caused by the discretization of the Navier–Stokes equation, which was solved based on the following equation [5, 14]:

$$\rho\left[\frac{\partial u}{\partial t}+(u.\nabla)u\right]=-\nabla p+\mu\nabla^2 u \qquad (11)$$

where $t$ is the time. In this work, the fluid dynamic viscosity and density were set to $10^{-6}$ m$^2$/s and 999.8 kg/m$^3$, respectively [15]. The simulation results are further presented and discussed in the following section. All the analyses were carried out with a *Re* values ranging from 10 to 100, which are suitable for biomedical applications.

## IV. Results and Discussion

The diffuser and nozzle losses as well as the efficiency of the diffuser were investigated while manipulating the geometry of the diffuser at different *Re* values. Initially, $\theta$ was varied at different *Re* values while observing the efficiency of the diffuser, as shown in Fig. 2. From the figure, it can be seen that the optimal diffuser angle that results the highest efficiency varies with the values of *Re* due to the flow circulation and separation, which is further explained in Fig. 5. Thus, this issue should be considered when designing a diffuser that is intended to be operated at a specific range of *Re*. In this case, it can be noticed that the optimal angle is within the range of 8 - 18°, resulting that the optimum angle for this range is usually set to 10° since it is more suitable for a wider range of *Re* values with the lowest variance in efficiency ratio evaluation [15].

Another analysis was carried out by fixing *Re* at 100 while varying the curvature ratio and angle of the diffuser, as shown in Fig. 3. The results agree with the ones presented in Fig. 2, where the highest efficiency is observed to be achieved at θ = 10° at the whole curvature ratio range, with the highest efficiency achieved at *CR* = 0.4. A further look into Fig. 3 shows that the maximum efficiency is affected by the diffuser angle, where the optimal curvature ratio for each angle is observed to increase accordingly with the value of the angle of the diffuser.

In addition, the length and angle of the diffuser were varied at the same Reynolds number value (100) while observing the efficiency of the diffuser, as illustrated in Fig. 4. It can be noticed that the length of the diffuser has a positive effect on the efficiency of the diffuser at all angle values, except at $\theta$ = 0°, where no significant effect is observed. However, a significant improvement in the efficiency is noticed at other diffuser angle values, especially < 40°. This relationship between the efficiency and length is caused by the change in the hydraulic diameter as the length varies, which will therefore affect the velocity of the fluid inside the diffuser (refer to (10)) [16]. Nevertheless, increasing the length of the diffuser beyond certain limits is not a practical solution in most cases, especially in microfluidic biomedical devices, where the reducing the size of the device is a crucial design factor. Thus, an effective diffuser length with a sufficient efficiency should be considered when designing such devices.

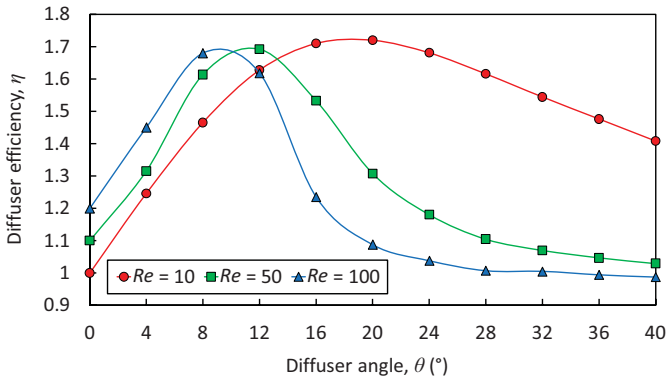


Fig. 2. Efficiency of the diffuser at different angles and Reynolds number values.

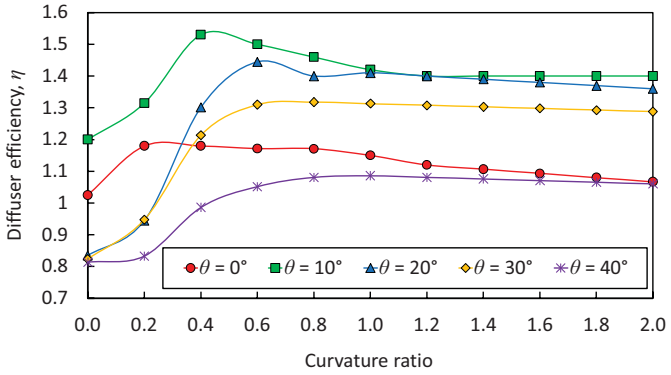


Fig. 3. Efficiency of the diffuser at different curvature ratios and angles at *Re* = 100.

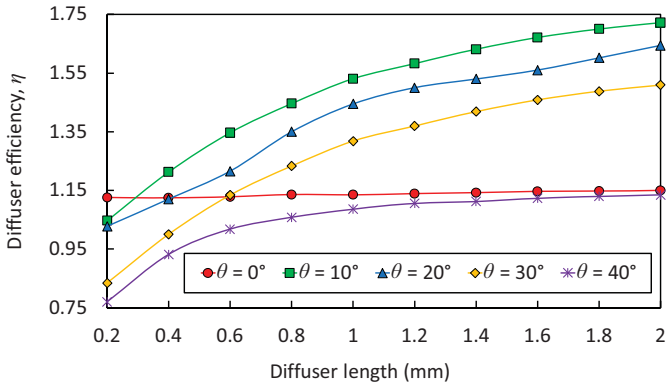


Fig. 4. Efficiency of the diffuser at different lengths and angles at *Re* = 100.

Finally, to understand the impact of the angle of the diffuser on the pressure coefficient and efficiency of the diffuser (refer to 6 and 8), the flow fields at different diffuser angles are illustrated in Fig. 5. The length and Reynolds number values were set to 1 mm and 100, respectively, while varying the angle to be 10, 20, 30, and 40°. At small diffuser angles (Fig. 5(a)), no flow separation is observed in the diffuser. However, increasing the diffuser angle beyond 10° causes a small flow separation at one-third of the length of the diffuser (Fig. 5(b)). Further increment in the diffuser angle causes the flow separation to move towards the entrance of the diffuser and

procedures a larger circulation zone on the walls (Fig. 5 (c) and (d)). At small diffuser angles, there is a high-pressure recovery and low flow separation in the diffuser direction, and vice versa in the nozzle direction, where the total losses are higher in the nozzle direction compared to the diffuser direction [17]. Such behavior explains the results presented in Fig. 2.

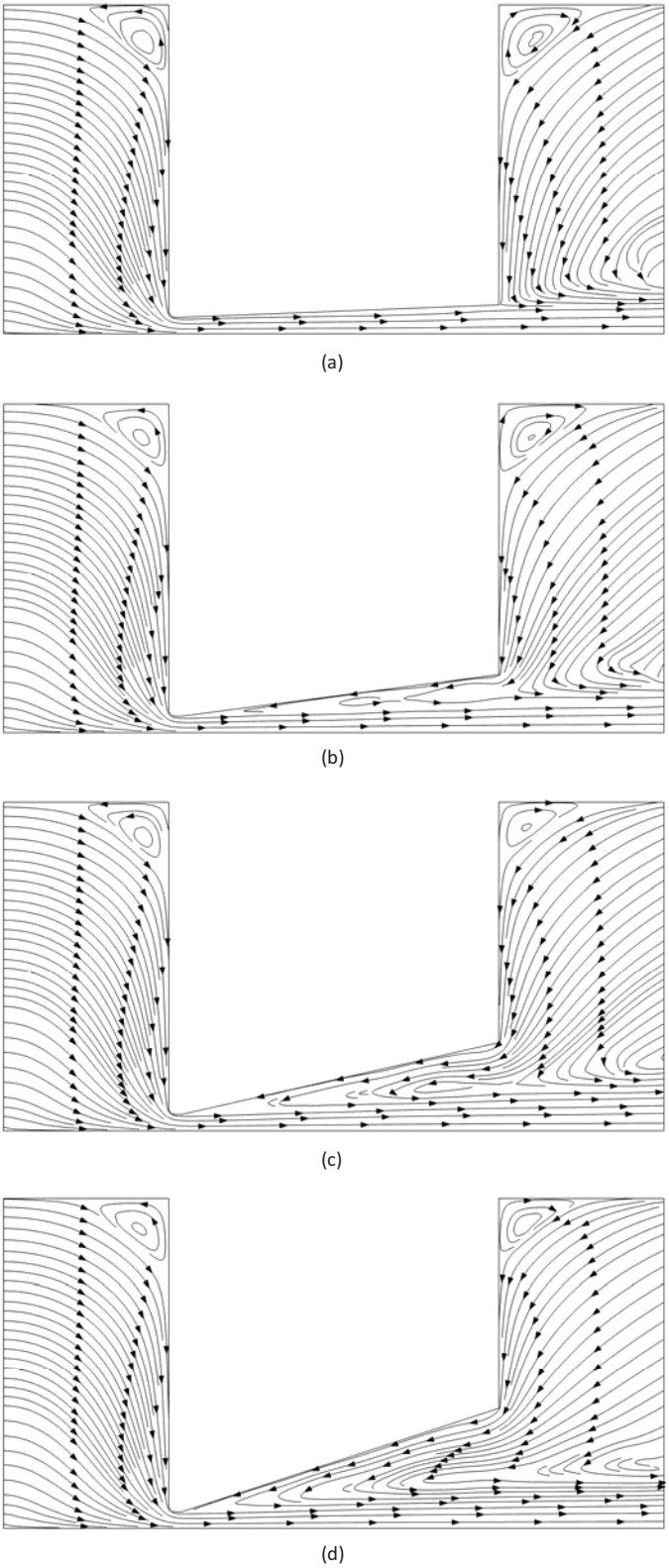


Fig. 5. Flow fields along the symmetry axis at $Re$ = 100 and $L$ = 1 mm for: (a) $\theta$ = 10, (b) $\theta$ = 20, (b) $\theta$ = 30, and (b) $\theta$ = 40.

## V. Conclusion

This paper presented a geometrical tuning for diffuser-nozzle elements for valveless micropumps. Several finite element analysis studies were carried out to examine the effect of the angle, curvature ratio, and length of the diffuser on the pumping efficiency. The simulation was performed via COMSOL Multiphysics® at Reynolds number values ranging from 10 to 100 while observing the pressure coefficients in the nozzle and diffuser directions, as well as the flow separation and the resultant efficiency of the diffuser. The results demonstrated that the diffuser with an angle of 10° and a curvature ratio of 0.4 possesses the highest efficiency among the other diffusers within the Reynolds number range of this study. In addition, it was observed that the efficiency of the diffuser was increased accordingly with the length of the diffuser. The reported results can be sued as designing guidelines for diffusers elements used in microfluidic devices for various biomedical applications. Further improvements could be made by studying a three-dimensional model of the diffuser and considering other geometrical factors, such as the height, slenderness, and area ratio. Future work will involve utilizing other methods to optimize the geometry of the diffuser, such as metamodel-based and particle swarm optimization methods [18].

## References

[1] A. Nisar, N. Afzulpurkar, B. Mahaisavariya, and A. Tuantranont, "MEMS-based micropumps in drug delivery and biomedical applications," *Sens. Actuators, B,* vol. 130, pp. 917-942, 2008.

[2] M. Nafea, A. AbuZiater, O. Faris, S. Kazi, and M. S. Mohamed Ali, "Selective wireless control of a passive thermopneumatic micromixer," in *2016 IEEE 29th International Conference on Micro Electro Mechanical Systems (MEMS)*, Shanghai, China, 2016, pp. 792-795.

[3] X. He, J. Shi, H. Yang, N. Lin, and B. B. Uzoejinwa, "Investigations on performance of valveless piezoelectric micropump with concave tuning diffuser/nozzle elements in transient flow," *Micro Nano Lett,* vol. 14, pp. 765-770, 2019.

[4] K.-S. Yang, T.-F. Chao, I. Y. Chen, C.-C. Wang, and J.-C. Shyu, "A comparative study of nozzle/diffuser micropumps with novel valves," *Molecules,* vol. 17, pp. 2178-2187, 2012.

[5] M. Nafea, N. Ahmad, A. R. Wahap, and M. S. Mohamed Ali, "Modeling and simulation of a wireless passive thermopneumatic micromixer," in *Communications in computer and information science book series*. vol. 751, M. S. Mohamed Ali, H. Wahid, N. A. Mohd Subha, S. Sahlan, M. A. Md. Yunus, and A. R. Wahap, Eds. Singapore: Springer Singapore, 2017, pp. 312-322.

[6] P. S. Chee, M. Nafea, P. L. Leow, and M. S. M. Ali, "Thermal analysis of wirelessly powered thermo-pneumatic micropump based on planar LC circuit," *J. Mech. Sci. Technol.,* vol. 30, pp. 2659-2665, 2016.

[7] M. Nafea, A. A. Badrul Hisham, N. A. Abdul-Kadir, and F. K. Che Harun, "Brainwave-controlled system for smart home applications," in *2018 2nd International Conference on BioSignal Analysis, Processing and Systems (ICBAPS)*, Kuching, Malaysia, 2018, pp. 75-80.

[8] Y. Liu, H. Komatsuzaki, S. Imai, and Y. Nishioka, "Planar diffuser/nozzle micropumps with extremely thin polyimide diaphragms," *Sens. Actuators, A,* vol. 169, pp. 259-265, 2011.

[9] M. Nafea, A. AbuZaiter, S. Kazi, and M. S. Mohamed Ali, "Frequency-controlled wireless passive thermopneumatic micromixer," *J. Microelectromech. Syst.,* vol. 26, pp. 691-703, 2017.

[10] Y. Guan and X. Li, "Analysis of vibrational performance of a piezoelectric micropump with diffuse/nozzle microchannel," *Nanotechnology and Precision Engineering,* vol. 1, pp. 138-144, 2018.
[11] A. Chandrasekaran and M. Packirisamy, "Geometrical tuning of microdiffuser/nozzle for valveless micropumps," *J. Micromech. Microeng.,* vol. 21, p. 045035, 2011.
[12] Y.-C. Wang, J.-C. Hsu, P.-C. Kuo, and Y.-C. Lee, "Loss characteristics and flow rectification property of diffuser valves for micropump applications," *Int J Heat Mass Transf,* vol. 52, pp. 328-336, 2009.
[13] M. Nafea, A. Nawabjan, and M. S. Mohamed Ali, "A wirelessly-controlled piezoelectric microvalve for regulated drug delivery," *Sens. Actuators, A,* vol. 279, pp. 191-203, 2018.
[14] B. Schmandt and H. Herwig, "Diffuser and nozzle design optimization by entropy generation minimization," *Entropy,* vol. 13, pp. 1380-1402, 2011.
[15] M. Nafea, J. Baliah, and M. S. M. Ali, "Modeling and simulation of a wirelessly-powered thermopneumatic micropump for drug delivery applications," *Indonesian Journal of Electrical Engineering and Informatics (IJEEI),* vol. 7, pp. 182-189, 2019.
[16] K.-S. Yang, I.-Y. Chen, B.-Y. Shew, and C.-C. Wang, "Investigation of the flow characteristics within a micronozzle/diffuser," *J. Micromech. Microeng.,* vol. 14, pp. 26-31, 2003.
[17] Y.-Y. Tsui and S.-L. Lu, "Evaluation of the performance of a valveless micropump by cfd and lumped-system analyses," *Sens. Actuators, A,* vol. 148, pp. 138-148, 2008.
[18] M. Nafea, C. Schlosser, S. Kazi, Z. Mohamed, and M. S. Mohamed Ali, "Optimal two-degree-of-freedom control for precise positioning of a piezo-actuated stage," *International Journal of Integrated Engineering,* vol. 9, pp. 93-102, 2017.